Materials Today Chemistry 17 (2020) 100285

Contents lists available at ScienceDirect

Materials Today Chemistry

journal homepage: www.journals.elsevier.com/materials-today-chemistry/

Bioinspired synthesis of multifunctional silver nanoparticles for enhanced antimicrobial and catalytic applications with tailored SPR properties

S.B. Parit [a], V.C. Karade [b], R.B. Patil [c, *], N.V. Pawar [a], R.P. Dhavale [d], M. Tawre [e], K. Pardesi [f], U.U. Jadhav [e], V.V. Dawkar [f], R.S. Tanpure [g], J.H. Kim [b], J.P. Jadhav [h], A.D. Chougale [a, **]

[a] The New College, Kolhapur, Shivaji University, Kolhapur, India
[b] Optoelectronic Convergence Research Center and Department of Materials Science and Engineering, Chonnam National University, Gwangju, 500-757, South Korea
[c] Yashwantrao Patil Science College, Solankur, Shivaji University, Kolhapur, India
[d] Department of Materials Science and Engineering, Yonsei University, South Korea
[e] Department of Microbiology, Savitribai Phule Pune University, Pune, India
[f] Biotechnology and Pharma Division, MITCON Foundation, Pune, India
[g] Biochemical Division, National Chemical Laboratory, CSIR, Pune, India
[h] Department of Biochemistry, Shivaji University, Kolhapur, India

ARTICLE INFO

Article history:
Received 30 March 2020
Received in revised form
19 April 2020
Accepted 20 April 2020
Available online xxx

Keywords:
Ag NPs
Gardenia resinifera
Antibacterial
Catalytic activity
Surface plasmon resonance

ABSTRACT

In the developing nanotechnology world, numerous attempts have been made to prepare the nobel metallic nanoparticles (NPs), which can improve their applicability in diverse fields. In the present work, the biosynthesis of silver (Ag) NPs has been successfully achieved through the medicinal plant extract (PE) of *G. resinifera* and effectively used for the catalytic and antibacterial applications. The size dependant tuneable surface plasmon resonance (SPR) properties attained through altering precursor concentrations. The X-ray and selected area diffraction pattern for Ag NPs revealed the high crystalline nature of pure Ag NPs with dominant (111) phase. The high-resolution TEM images show the non-spherical shape of NPs shifting from spherical, hexagonal to triangular, with wide particle size distribution ranging from 13 to 44 nm. Accordingly, the dual-band SPR spectrum is situated in the UV–Vis spectra validating the non-spherical shape of Ag NPs. The functional group present on the Ag NPs surface was analysed by FT-IR confirms the capping and reducing ability of methanolic PE *G. resinifera*. Further, the mechanism of antimicrobial activity studied using electron microscope showed the morphological changes with destructed cell walls of *E. coli* NCIM 2931 and *S. aureus* NCIM 5021 cells, when they treated with Ag NPs. The Ag NPs were more effective against *S. aureus* and *E. coli* with MIC 128 μg/ml as compared to *P. aeruginosa* NCIM 5029 with MIC 256 μg/ml. Apart from this, the reduction of toxic organic pollutant 4-NP to 4-AP within 20 min reveals the excellent catalytic activity of Ag NPs with rate constant k = 15.69 s^{-1}.

1. Introduction

Nanoscience and nanotechnology are now becoming the mainstream of the developing world, through upscaling and modernizing the fabrication, design and physicochemical assets of nanomaterials [1,2]. The use of nanomaterials reached skyrocket in daily life, as they found numerous applications in the field of food, chemical industries, catalyst, optoelectronics, environmental health, energy science, drug delivery, cosmetics, biomedical sciences and so on [3–10]. However, some properties of nanomaterials limit their applicability and usage in a different field, hence the developing multifunctional nanomaterials are always been a challenging task. Recently different metal and metal oxides-based nanomaterials such as nanoparticles (NPs), nanotubes, dendrimers have emerged as the potential multifunctional

* Corresponding author.
** Corresponding author.
E-mail addresses: rrahulpatil@gmail.comm (R.B. Patil), ashokdchougale@gmail.comm (A.D. Chougale).

https://doi.org/10.1016/j.mtchem.2020.100285
2468-5194/

nanomaterials [11–13]. Among them nobel metal NPs like silver (Ag), gold, palladium and platinum have proved their applicability in different fields like antibacterial, SERS, catalysis, supercapacitor, gas sensing, etc. For Ag NPs several emerging applications in paints, as an antioxidant, an anticoagulant in thrombolysis besides as the larvicidal agent have been reported [14–16]. Additionally, it was anticipated that biogenic Ag NPs can induce apoptosis, generate reactive oxygen species (ROS) and switch on the apoptotic signalling pathway in the cancerous cell, which has also widened their scope in the anticancer agents and drug delivery systems [17–21].

Concerning antimicrobial activity, finding the antibiotic resistance strategy is highly important and is the primary challenge for the research community. Recent studies show that some metal NPs maintain antimicrobial activity and give less toxicity, overcoming the resistance along with a lower cost [22,23]. Therefore compared to the small antibiotic molecule, they can last longer in the body and thus be useful for sustained therapeutic effects [24]. Ag ions are susceptible to yeast, fungi, viruses and a wide range of anaerobic, aerobic, gram-positive and gram-negative bacteria. The term used for silver 'oligodynamic' reveals that the small amount is sufficient for its action [25]. Consequently, Ag NPs are also referred to as the most powerful nano-weapon combating bacterial infections.

Environmental pollution is also one of the major issues, due to industrial effluent. Nitrophenols are one of the organic pollutants largely found in agriculture and industrial waste. Hence, the degradation of the 4-NP to 4-AP makes it safer and starting material for the pharmaceutical and dye industry. Some chemicals having nitro, chloro groups or derivatives of phenols e.g. p-nitrophenol (PNP, 4-nitrophenol, 4-NP) intensify their toxicity to the human being for the occurrence of phenol group [26]. The PNP can have diseases like cyanosis, inflammation allergies. Thus, it is necessary to find a solution to the degradation of industrial effluent. Recently different NPs based catalysts have been successfully introduced for the reduction of industrial effluents owing to their high surface to volume ratio, high selectivity and improved structural properties [27–30]. In catalyses also, Ag NPs have received significant attention owing to their excellent catalytic activity designed for chemical reductions, which also includes the reduction from 4-NP to 4-AP [31–36].

So, to use these Ag NPs in various applications different synthesis techniques have been developed [37]. However, compared with chemical and physical methods of synthesis, biogenic synthesis of metal NPs using medicinal plant extracts or microorganisms is an eco-friendly solution. Besides, one can also use the naturally available abundant agro-waste or arthropods resources during synthesis, as they consist of a large number of active biomolecules like proteins, phenols, flavonoids and metabolites which may act as capping and reducing agents during synthesis process [38–41]. Green route is the kind of bottom-up process in which the oxidation and reduction reactions are used to produce NPs where the plant extract itself acts as a stabilizing agent. For materials synthesis, the green synthesis of NPs has become a significant method [42]. The essentiality of the green route arose due to expensive and toxic chemicals used during the synthesis process. Frequently during chemical synthesis, the presence of some toxic chemicals gets absorbed on the surface which is not ideal for the medical application of NPs. The awareness about the environment leads to an emphasis on the green route, using non-toxic chemicals, renewable materials, eco-friendly reactions. The Ag NPs synthesized using medicinal plant extracts can serve as cargo for delivering active compounds of the plants with enhanced stability and intestinal permeability. To date, few medicinal plants have been used for the synthesis of Ag NPs which are biologically active against MDR pathogens [43–46].

Herein we report, the successful green synthesis of Ag NPs from the medicinal plant extract (PE) of *G. resinifera* and its different applications. In this work, the methanolic PE of *G. resinifera* has been used along with silver nitrate as a precursor for producing Ag NPs. The *G. resinifera* is a key plant from a medicinal point of view. The nature of the capping agent plays a vital role in the antimicrobial performance of Ag NP. Here, *G. resinifera* itself acted as a capping and reducing agent. The size and shape dependent tunable SPR properties are explored in detail. Besides, the preparation, characterization and size-shape specific antimicrobial efficacy along with the catalytic activity of Ag NPs are reported. A facile, one-pot green synthesis for the generation of Ag NPs over a wide size range has been achieved by altering different preparative parameters.

2. Experimental methods

2.1. Preparation of plant extract

The *gardenia* leaves were gently washed initially under tap water and then deionized (DI) water. The washed leaves were dried at 40 °C with the help of the oven and further converted to powder form. The 5% extract was prepared using methanol (100 mL) and *G. resinifera* powder (5 gm). Finally, methanolic extract was stored at room temperature for further use.

2.2. Biosynthesis of silver nanoparticles

Silver nitrate ($AgNO_3$) is one of the best-known sources of ionic silver. Reduction of Ag^+ to Ag^0 was carried out by mixing 50 mL *gardenia* leaf extract dropwise in 50 mL of 10 mM $AgNO_3$ with stirring at 200 rpm for 5 h in dark at room temperature. The impact of Ag^+ ion concentration on the formation of Ag NP was estimated by changing the concentration of $AgNO_3$ to 1, 5 and 10 mM. The green-colored solution of $AgNO_3$ and PE changes to dark brown and further to dark black after time intervals. The change in color indicates the formation of Ag NPs. The reduction kinetics was observed in the visible range by UV–Vis absorption spectroscopy. The AgNPs were collected after centrifugation (10,000 rpm, 2hr) process. It was further washed to remove excess PE and unreacted precursor. The concentrated solution of Ag NP was then dried at 40 °C and was used for further study.

Further detailed information about the part of the applications is provided in the supplementary information.

3. Result and discussions

3.1. X-ray diffraction study

The surface to volume ratio and the crystallographic structures of NPs plays an important role in determining the activity of Ag NPs [47]. The diffraction spectra of Ag NPs prepared at different concentration is shown in Fig. 1. As can be seen in the figure the orientation and growth of crystals differ with precursor concentrations. Besides, the crystallinity of NPs gets strongly influenced by the initial precursor concentrations. The prepared Ag NPs exhibits fcc crystalline structure, at lower concentrations the (1 2 2) and (2 3 1) planes have their predominant nature, whereas at higher concentrations (1 1 1), (2 0 0), (2 2 0) and (3 1 1) planes shows strong intensity peak at respective 2θ values coinciding with data sheet 04–0783. The similar diffraction peaks for Ag NPs were also observed by Prasannaraj et al. [48]. Some unidentified crystalline peaks at 46.02° and 57.19° were also observed, these unidentified crystalline peaks are also obvious in many works in the relevant 2θ range due to the organic compounds present in the plant extract

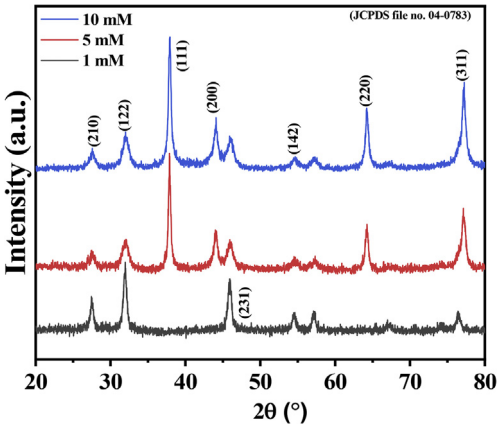

Fig. 1. XRD spectra of Ag NPs synthesized at different precursor concentrations.

[49–51]. The wider peaks with smaller intensity and some strong peaks indicate the altered particles size with the increase in precursor concentrations. Further the size and shape of Ag NPs were confirmed with HR-TEM studies.

3.2. Morphology analysis

The size and morphology of Ag NPs were examined by HR- TEM. Fig. 2(a)–(c) shows low magnification TEM images and Fig. 2(d)–(f) shows high magnification images of Ag NPs synthesized at different precursor concentrations. It was observed that the size of the Ag NPs found to increase with increased precursor concentration Fig. 2(a)–(c). The increased precursor concentration might have caused the agglomeration of NPs giving rise to the increased crystalline size which is consistent with diffraction data. The NPs size histogram obtained from Fig. 2 is represented in Fig. S1. At low concentration, the average NPs size is about 13 nm, whereas it augmented to 40 and 44 nm at 5 mM and 10 mM concentrations respectively. The high magnification images of Ag NPs revealed uneven morphology, fluctuating from very small spherical shape to larger non-spherical shape, especially hexagonal then to triangular shape Fig. 2(d)–(f) respectively. The conventional Ag NPs growth typically involves the rapid reduction of precursors Ag^{+} ion through a heat process, resulting in spherical or pseudospherical NPs such as cuboctahedrons and icosahedrons [52]. However present work involved the clean and non-toxic approach for synthesizing Ag NPs lacking the external heating processes. This factor might influence the room temperature growth of Ag NPs resulting in the size and shape fluctuations. The selected area electron diffraction (SAED) pattern of Ag NPs obtained from HR-TEM images exhibited concentrated rings which suggest the increased crystallinity with precursor concentration showing the polycrystalline nature which is consistent with the XRD results Fig. 2(h)–(i). However, in case of the first sample i.e. at a low concentration of $AgNO_3$ (1 mM) it was difficult to examine the SAED pattern since it can be seen in Fig. 1 the diffraction peaks have low intensity defining low crystallinity. Except for the planes (1 1 1), (2 0 0) and (2 2 0) rest of the planes coincides with the fcc structure of Ag NPs find in XRD. The most effective geometry of Ag NPs towards antimicrobial efficacy has been non-spherical i.e. truncated triangular shape [23,33], which was used for further study in the antibacterial application. The zeta potential was also measured to evaluate the particle surface charge and shown in Fig. S2. The synthesized Ag NPs with a 5 mM concentration surface carries the Zeta potential of − 13.9 mV.

3.3. SPR analysis

In the present study, the fixed concentration 5% of the PE of *G. resinifera* was added to the 1, 5 and 10 mM $AgNO_3$ precursors. As the extract was added in precursor the initial green color of the reaction mixture immediately turn in to dark brown and further to the intense black. These visual changes are attributed to the fast change of the SPR from Ag NPs, for the reduction of Ag^{+} ions to metallic Ag^{0} state or Ag NPs. Further, the UV–Visible spectroscopy was used to illustrate the SPR properties of prepared Ag NPs. As the appearance of an SPR band is the result of the interaction between incident light from the NPs surface with the conduction electrons of the metal [52]. The resonant frequency of superficial plasmons strongly depends on the size and shape of NPs, giving an effective way of evaluating optical properties.

Fig. 3 shows the UV–Visible spectrum of Ag NPs prepared at different precursor concentrations. The spectrum shows two distinct peaks around 363 and 426 nm. A vibrant SPR band at ~426 seen in the figure, which is the characteristic SPR peak for Ag, indicates the successful synthesis of Ag NPs. This peak can be assigned to the dipole resonance among Ag NPs. It can be seen that the peak intensity decreases as a function of precursor concentration. For 1 mM $AgNO_3$, the intensity is lowest whereas it is highest for 10 mM concentration. The highest SPR intensity suggests that the number of Ag NPs has reached the maximum, indicating the completion of the reaction. At the same time, it should be noted that no significant peak shift is observed for change in concentration. This behavior may indicate the rapid bioreduction of Ag^{+} ions. It is known that, when Ag clusters start to grow as a particle, they develop an optical absorption band contingent to the SPR of their free electrons and further give strong resonance for enhanced NPs size [53,54]. Similarly, careful observation reveals shoulder at ~455 nm denoting the heterogeneous size distribution of Ag NPs. It was observed that the SPR band occurs initially at 422 and after the complete reaction, the SPR band stabilizes at 430 nm. This peak is attributed to the presence of spherical shaped Ag NPs. The bump for higher concentration and broadening of the peak width indicates the aggregation of smaller NPs causing an increase in the NPs size. Another SPR peak at 363 nm can be seen for all the cases, this SPR is present in all cases irrespective of NPs size. The peak positions remained constant and peak intensity found to increase with increased precursor concentrations complies the increased NPs size.

As per Mie's theory, only a single band is expected in the absorption spectra of spherical NPs. According to Kerry et al. [54], the plasmon resonance depends strongly on the NPs shape. Sun et al. [55] reported a strong SPR band at 430 nm for spherical NPs, whereas three SPR bands at 350, 400 and 470 nm for cubic NPs (having edge length ~ 80 nm). From these reports, it is clear that the position and number of bands strongly depend on the size and shape of the Ag NPs and hence verified in the present work. The newly appearing peak can be thus assigned to non-spherical shape and quadrupole resonance. Few reports suggest that the band at ~350 nm is due to transition involving higher multipoles of Ag NPs [56,57]. This multipole transition becomes more prone to the NPs having symmetry less than a sphere. According to Amendola et al. [58], SPR of Ag NPs can be tuned and the number of peaks depends on the shape of Ag NPs. It suggests a single SPR band for spherical NPs, while two or more for reduced symmetry. Isolated Ag spheres exhibit unique plasmonic resonance because of their symmetry, nevertheless, additional resonances may appear when they are ordered in small assemblies. The present work also validates the proposed theory with different shapes from spherical to triangular.

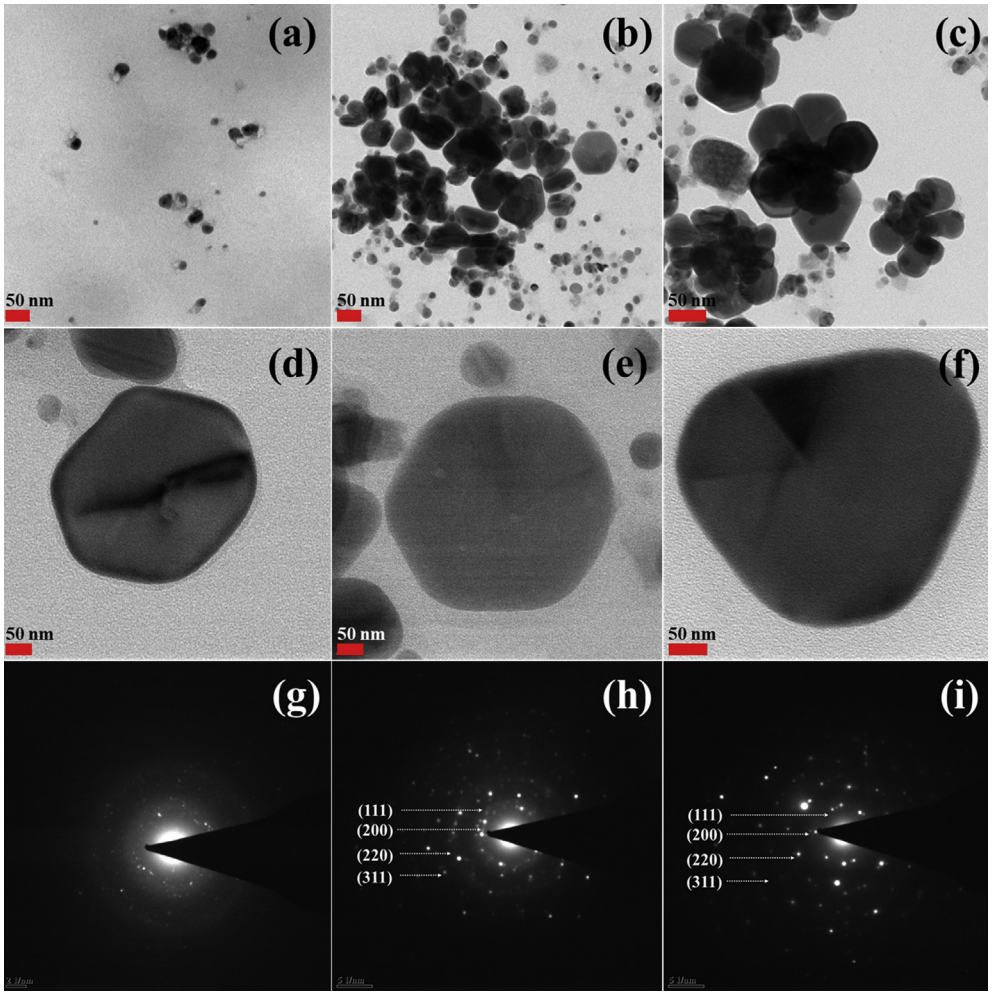

Fig. 2. TEM images of Ag NPs synthesized at (a) 1 mM, (b) 5 mM and (C) 10 mM concentration, respective high resolution well-grown non-spherical shapes at (d) 1 mM, (e) 5 mM and (f) 10 mM concentration and corresponding SAED patterns for (g) 1 mM, (h) 5 mM and (i) 10 mM concentration respectively.

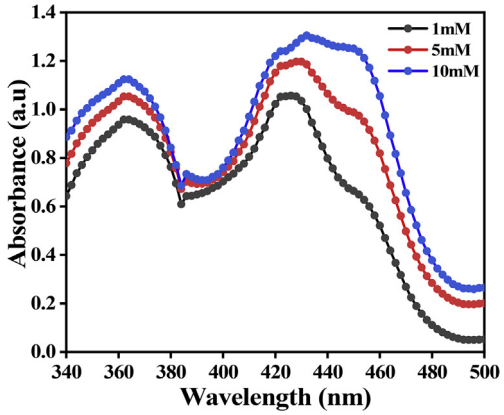

Fig. 3. UV–Visible spectra of Ag NPs synthesized at different concentrations from *G. resinifera* extract.

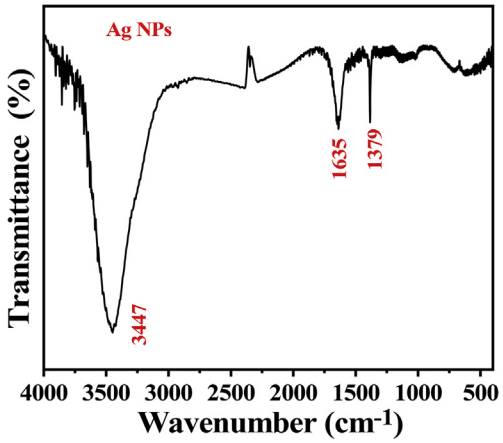

Fig. 4. FTIR spectra of Ag NPs synthesized from *G. resinifera*.

3.4. FTIR analysis

The dual role of PE as a capping and reducing agent along with the presence of functional groups of Ag NPs was confirmed by FTIR. Fig. 4 shows the FTIR spectra of Ag NPs.

The participation of these contents in the reduction and capping were revealed by the FTIR analysis. In our previous work, a similar *G. resinifera* plant extract was analyzed Fig. S3. The analysis confirmed the existence of terpenoids-phenols, phenolic acids, and aliphatic amines through the peaks for bending vibration of C—H, stretching vibration of C═O and stretching vibration of C—N

bonds, respectively [59]. Further, the vacuum-dried Ag NPs were subjected to FT-IR analysis and this study revealed different stretching bonds at 3447.28 cm^{-1}, 1635.28 $cm^{-1,}$ and 1379.79 $cm^{-1.}$ The −OH groups present in the metabolites like carboxylic acids were shown in the *G. resinifera* extract at 3300 cm^{-1} which gets shifted to 3452.80 cm^{-1} in Ag NPs. The existence of the phenolic groups in the PE and capping of the Ag NPs was confirmed by the response between the 1315–1037 cm^{-1} and 1456–1600 cm^{-1} region. Existence of −NH group confirms by peak value at 1635 cm^{-1} which may be from flavonoids appears on the AgNPs surface. It was observed that after the reduction of the Ag^{+} the peak values were shifted to higher values. A similar shift in the peaks was observed by Anandalakshmi et al. [55]. The flavonoids, amides and phenolic metabolites present in the methanolic extract of the *G. resinifera* having the reducing power involved in the conversion of Ag^{+} to Ag^{0}. The contents of the flavonoids and phenols of the methanolic extract of *G. resinifera* were studied and are reported in Table 1.

Additionally, the EDAX spectra acquired for all the Ag NPs show the peaks for the Ag, N, C, O elements (Figs. S4, S5, S6). The EDAX spectra support the FT-IR analysis and confirm the existences besides capping activity by amide and flavonoids group over the Ag NPs.

3.5. Antimicrobial activity

In general, the size and shape of NPs have a strong influence on antimicrobial activity. More precisely, when Ag NPs have 10–15 nm size they show better stability, biocompatibility and enhanced antimicrobial activity [60,61]. The truncated triangular shaped Ag NPs showed better antibacterial activity as compared to spherical or rod-shaped [42,47]. Ag NPs have been proved effective against over 650 microorganisms including bacteria (both gram-positive and negative), fungi and viruses [62]. Besides, the environment provided during activity can also have a significant impact on the inhibition pathway. Since experiments under visible light could enhance the anti-bacterial activity as the production of ROS is sensitive to plasmonic excitation [63].

Bactericidal properties of metallic Ag are associated with its slow oxidation and liberation of Ag^{+} ions to the environment [64]; hence, it seems promising to use nano-silver drugs as a special class of biocidal agents. In the present study, four microorganisms were chosen for the test are shown in Table 2. The *P. putida* (*PAW1*), *E. coli* and *P. aeruginosa* represent the gram-negative bacteria whereas *S. aureus* refers to gram-positive bacteria. The Ag NPs attached to the cell membranes cause a change in lipid bilayers which shows increased membrane permeability, damage and cell death [65]. Both classes of bacteria displayed complete growth inhibition at higher (>75 μg/ml) Ag NPs concentrations. The growth inhibition studies of Ag NPs against both gram-positive and gram-negative were carried out as shown in Table 2. Moreover, the digital photograph of culture plates showing successful antibacterial activity with inhibition zone is also shown in Fig. S7.

The inhibition zone against all the bacteria indicates the effectual antimicrobial action. The Ag NPs were more effective against *S. aureus* and *E. coli* with MIC 128 μg/ml as compared to *P. aeruginosa* with MIC 256 μg/ml. Antibacterial action of Ag NPs is more effective when NPs have a size lesser than 50 nm [66]. It is due to their superior penetration ability into the bacteria. El-Kheshen et al. [67] reported MIC 125 mg/ml for the citrate capped Ag NPs against *E. coli* ATCC 8739 strain for an initial bacterial concentration of 10^{5}–10^{6} CFU ml^{-1}. The Ag NP colloidal suspension has also been used by Taner et al. [68] for antibacterial purposes with a reported MIC of >150 mg/ml against *E. coli* DH5α strain at ~10^{8} CFU ml^{-1} initial bacterial concentration. Agnihotri et al. [69] reported MIC of 80–130 μg/ml against the *S. aureus* NCIM 5021 strain at 10^{5}–10^{6} CFU ml^{-1} initial bacterial concentrations. The positive surface charge of Ag^{+} ion confers electrostatic attraction between Ag NPs and negatively charged cell membranes of the microorganisms, thereby facilitates Ag NPs attachment onto cell membranes. The morphological changes become evident upon such interaction and can be characterized by shrinkage and membrane detachment finally leading to the rupture of the cell wall. The consistent morphology changes results of untreated *E. coli* and *S. aureus* cells as observed under FESEM was intact whereas after treatment with Ag NPs was found distorted as shown in Fig. 5.

The studies showed the morphological changes when *E. coli* and *S. aureus* cells were treated with Ag NPs. The *E. coli* and *S. aureus* cells treated by Ag NPs were found to shrank with distorted cell membranes as compared to untreated cells which were found to be smooth and intact. These results are in accordance with previous reports by Alsammarraie et al. [43] and Ali et al. [45]. The completely disrupted cell membrane of *E. coli* after treatment with Ag NPs has been reported by Raffi et al. [70]. The plausible mechanism for the antimicrobial action of Ag NPs is linked with four well-defined steps [71]. As (a) adhesion of Ag NPs on the surface cell wall and membrane; (b) penetration of Ag NPs inside the cell and damage the intracellular structure; (c) induced Ag NPs cellular toxicity and oxidative stress by reactive oxygen species (ROS) and free radicals; (d) modulation of signal transduction pathways. The inhibition of the growth in the case of *S. aureus* was less remarkable while *E. coli* was inhibited at low Ag NPs concentrations and *S. aureus* was less susceptible than *E. coli* [72]. The antimicrobial potential of Ag NPs is also influenced by the thickness and composition of the cell wall of the microorganisms. The gram-negative bacteria (such as *E. coli*) are more susceptible to Ag NPs than gram-positive bacteria (such as *S. aureus*). Thicker cell wall and negatively charged peptidoglycan leave Ag^{+} ions stuck onto the cell wall and hence gram-positive bacterium prevents the action of the Ag^{+} ions and renders more resistant to antimicrobial therapy of Ag NPs [72]. The gram-negative bacteria consist of negatively charged lipopolysaccharide (LPS) that promotes adhesion of Ag NPs and makes bacteria more susceptible to antimicrobial therapy [47].

Table 1
Phenolic and flavonoid content of *G. resinifera*.

	Solvents	TPC (mg/g±SE)	TFC (mg/g±SE)
Plant	Methanol	41.58 ± 0.07	29.42 ± 0.05
	Water	21.50 ± 0.04	28.18 ± 0.05

Table 2
Susceptibility of Ag NPs.

Test Microorganisms	Zone diameter (mm)	MIC (μg/ml)
S. aureus NCIM 5021	12	128
E. coli NCIM 2931	13	128
P. aeruginosa NCIM 5029	11	256
P. aeruginosa PAW1	11	128

3.6. Catalytic activity

Along with the bacterial activity, the catalytic performance of Ag NPs was also tested through a reduction reaction of 4-NP to 4-AP in the presence of $NaBH_4$. The Ag NPs provides the adsorption sites for BH_4 ions and hydrogen [64]. The Ag NPs catalyze the reduction reaction by facilitating the electron transfer process from the donor BH_4 ions to the acceptor 4-NP as illustrated in Fig. 6.

The reduction of the 4-NP to 4-AP can be monitored by a decreased absorption peak at 400 nm. The $NaBH_4$ acts as a reducing

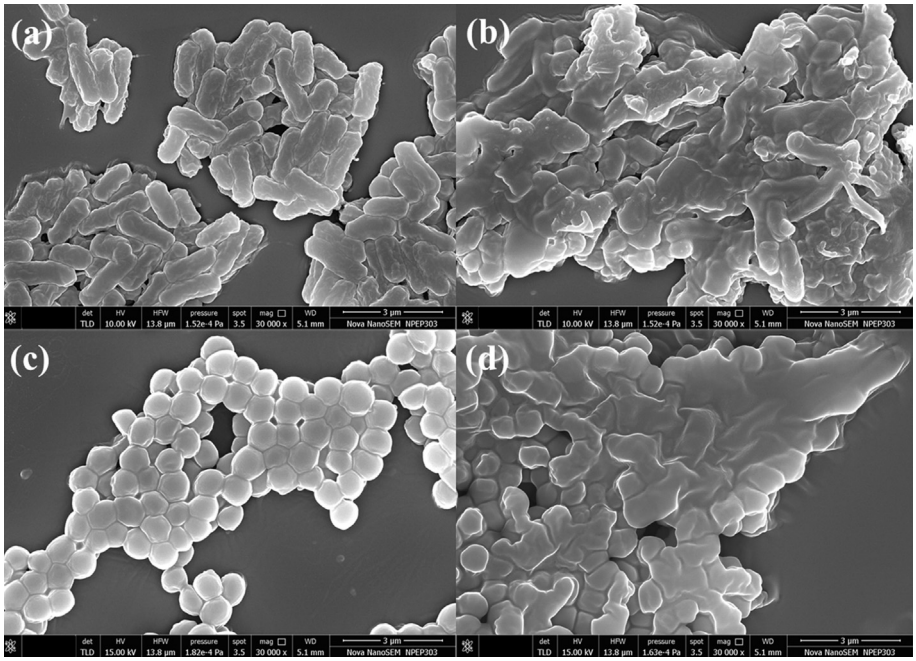

Fig. 5. Morphology of (a) untreated *E. coli* and (c) *S. aureus* (intact) cells, treated (b) *E. coli* and (d) *S. aureus* cells (distorted).

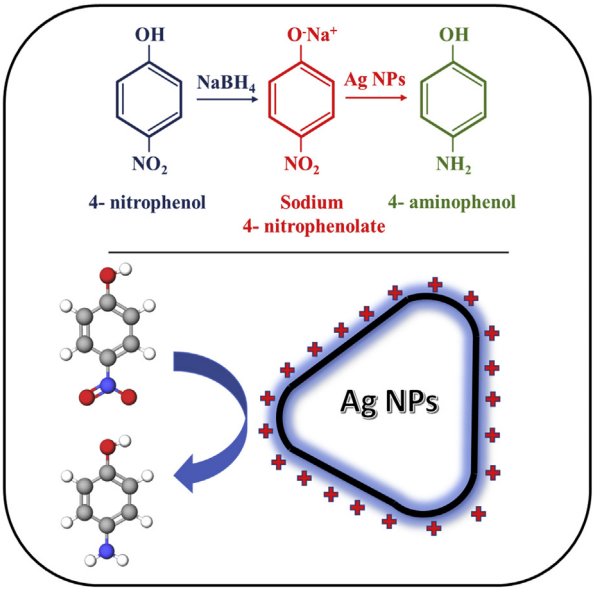

Fig. 6. Schematic mechanism of reduction of 4-NP to 4-AP.

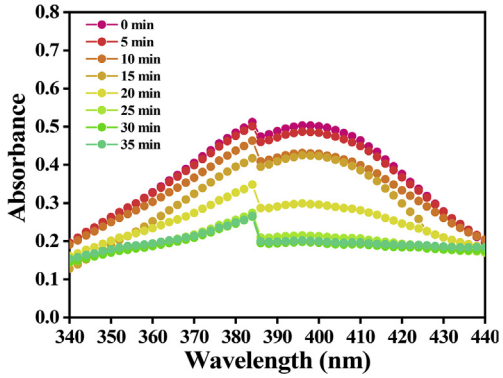

Fig. 7. The catalytic activity of Ag NPs synthesized from *G. resinifera*.

agent but the reduction rate is very slow and hence peak intensity become unchanged for a longer time [73]. However, up on addition of a small amount of Ag NPs, the reduction process occurred instantaneously. At the same time, the yellow color of 4-nitrophenolate changed to colorless, which also indicated the formation of 4-AP [74]. The hydrogen from $NaBH_4$ is adsorbed by the Ag NPs and releases it during the reduction reaction. The addition of catalyst accelerated the percentage of conversion of 4-NP to 4-AP which was monitored every 5 min. The reduction in the intensity of the absorption peak at 400 nm was observed which further disappeared after 20 min as shown in Fig. 7.

Based on the reduction catalytic activity of the Ag NPs the rate constant and half-life of reaction time was calculated using equation (1) respectively and shown in Fig. S8. Equation (1) signifies the behavior of ln (A/A_0) with respect to time:

$$\ln(A/A_0) = -kt \quad (1)$$

where Ao is the initial absorbance of the reaction system, A is the absorbance at time t, and k is the rate constant of the reaction. From equation (1) the reduction activity can be considered to be as pseudo-first-order type. Since there is a relative decrease in the intensity of characteristic absorption peak around 400 nm followed by the time. The rate constant k (s^{-1}) determined for reduction of 4-NP to 4-AP is about $k = 15.69\ s^{-1}$. From this it can be concluded that the green synthesized Ag NPs with variable shape can be a potential catalyst candidate for the room temperature reduction of 4-NP.

In the perspective briefly.

a) the as-synthesized multifunctional (i.e. antimicrobial and catalytic activity) Ag NPs may enhance its use in the wastewater treatment as well as in biomedical applications. Progressively, the Ag NPs will reduce the count of bacteria along with detoxifying the nitrophenols from the wastewater.

b) The Ag NPs can be used in combination with antibiotics which would enhance the activity and reduce the concentration of each (low dosage) and hence reduce toxicity. These Ag NPs are good candidates to treat wound infections and can be used in wound dressings or gel formulations.

4. Conclusions

The field of nanobiotechnology is looking for eco-friendly, cost-effective, green synthesis of medicinal plant extracted Ag NPs which offer biomedical applications. For the first time, a facile one-pot green approach to synthesize Ag NPs has been successfully done using *G. resinifera* which itself acted as reducing and capping agents. The synthesized Ag NPs had non-spherical shapes ranging from 13 to 44 nm depending upon the precursor concentration. The UV–Vis spectra and TEM analysis supported the heterogeneous combination of shapes of AgNPs. The dual SPR band is an optical signature of Ag NPs synthesized by using *G. resinifera* signifies the tailored SPR of Ag NPs. The phytochemical analysis of plant showed a higher concentration of phenolic and flavonoid content which involve rapid reduction and capping of Ag NPs supported by FT-IR and EDAX. In the application part, the Ag NPs were more effective against *S. aureus* and *E. coli* with MIC 128 μg/ml as compared to *P. aeruginosa* with MIC 256 μg/ml. Ag NPs were found effective against PAW1 a clinical wound isolates with MIC 128 μg/ml which confirm its potential antimicrobial feature. Proving their multifunctionality the Ag NPs shows enhanced catalytic activity with the conversion of toxic organic pollutant 4-NP to 4-AP in the presence of $NaBH_4$ within 20 min. The dual SPR band of Ag NPs synthesized by using *G. resinifera* a medicinal PE can be an imperative solution within biomedical applications of Ag NPs. This work opens the possibility of studying the generation of Ag nanostructures in a one-step inexpensive synthesis and with the possibility of getting different nonspherical morphologies at the same time.

Declaration of Competing Interest

The authors declare that they have no known competing financial interests or personal relationships that could have appeared to influence the work reported in this paper.

CRediT authorship contribution statement

S.B. Parit: Writing - original draft, Data curation. **V.C. Karade:** Writing - original draft, Data curation. **R.B. Patil:** Methodology, Conceptualization. **N.V. Pawar:** Visualization. **R.P. Dhavale:** Visualization. **M. Tawre:** Visualization. **K. Pardesi:** Visualization. **U.U. Jadhav:** Visualization. **V.V. Dawkar:** Writing - review & editing. **R.S. Tanpure:** Visualization. **J.H. Kim:** Writing - review & editing. **J.P. Jadhav:** Supervision. **A.D. Chougale:** Methodology, Conceptualization.

Acknowledgment

This work was supported by the Human Resources Development Program (No. 20194030202470) of the Korea Institute of Energy Technology Evaluation and Planning (KETEP) Grant funded by the Korean Government Ministry of Trade, Industry and Energy.

Appendix A. Supplementary data

Supplementary data to this article can be found online at https://doi.org/10.1016/j.mtchem.2020.100285.

References

[1] F. Salamanca-Buentello, D.L. Persad, E.B. Court, D.K. Martin, A.S. Daar, P.A. Singer, Nanotechnology and the developing world, PLoS Med. 2 (2005) e97, https://doi.org/10.1371/journal.pmed.0020097.
[2] F.J. Heiligtag, M. Niederberger, The fascinating world of nanoparticle research, Mater. Today 16 (2013) 262–271, https://doi.org/10.1016/j.mattod.2013.07.004.
[3] N.G. Bastús, F. Merkoçi, J. Piella, V. Puntes, Synthesis of highly monodisperse citrate-stabilized silver nanoparticles of up to 200 nm: kinetic control and catalytic properties, Chem. Mater. 26 (2014) 2836–2846, https://doi.org/10.1021/cm500316k.
[4] P. Sutradhar, M. Saha, Silver nanoparticles: synthesis and its nanocomposites for heterojunction polymer solar cells, J. Phys. Chem. C 120 (2016) 8941–8949, https://doi.org/10.1021/acs.jpcc.6b00075.
[5] P. Raveendran, J. Fu, S.L. Wallen, Completely "green" synthesis and stabilization of metal nanoparticles, J. Am. Chem. Soc. 125 (2003) 13940–13941, https://doi.org/10.1021/ja029267j.
[6] N. Tarannum, Divya, Y.K. Gautam, Facile green synthesis and applications of silver nanoparticles: a state-of-the-art review, RSC Adv. 9 (2019) 34926–34948, https://doi.org/10.1039/c9ra04164h.
[7] S.H. Lee, B.H. Jun, Silver nanoparticles: synthesis and application for nanomedicine, Int. J. Mol. Sci. 20 (2019), https://doi.org/10.3390/ijms20040865.
[8] I. Khan, K. Saeed, I. Khan, Nanoparticles: properties, applications and toxicities, arab, J. Chem. 12 (2019) 908–931, https://doi.org/10.1016/j.arabjc.2017.05.011.
[9] H.D. Beyene, A.A. Werkneh, H.K. Bezabh, T.G. Ambaye, Synthesis paradigm and applications of silver nanoparticles (AgNPs), a review, Sustain. Mater. Technol. 13 (2017) 18–23, https://doi.org/10.1016/j.susmat.2017.08.001.
[10] A.C. Burduşel, O. Gherasim, A.M. Grumezescu, L. Mogoantă, A. Ficai, E. Andronescu, Biomedical applications of silver nanoparticles: an up-to-date overview, Nanomaterials 8 (2018), https://doi.org/10.3390/nano8090681.
[11] J. Jeevanandam, A. Barhoum, Y.S. Chan, A. Dufresne, M.K. Danquah, Review on nanoparticles and nanostructured materials: history, sources, toxicity and regulations, Beilstein J. Nanotechnol. 9 (2018) 1050–1074, https://doi.org/10.3762/bjnano.9.98.
[12] H. Tabassum, A. Mahmood, B. Zhu, Z. Liang, R. Zhong, S. Guo, R. Zou, Recent advances in confining metal-based nanoparticles into carbon nanotubes for electrochemical energy conversion and storage devices, Energy Environ. Sci. 12 (2019) 2924–2956, https://doi.org/10.1039/c9ee00315k.
[13] Y.H. Wang, L.L. He, K.J. Huang, Y.X. Chen, S.Y. Wang, Z.H. Liu, D. Li, Recent advances in nanomaterial-based electrochemical and optical sensing platforms for microRNA assays, Analyst 144 (2019) 2849–2866, https://doi.org/10.1039/c9an00081j.
[14] A. Lateef, M.A. Akande, S.A. Ojo, B.I. Folarin, E.B. Gueguim-Kana, L.S. Beukes, Paper wasp nest-mediated biosynthesis of silver nanoparticles for antimicrobial, catalytic, anticoagulant, and thrombolytic applications, 3 Biotech (2016) 6, https://doi.org/10.1007/s13205-016-0459-x.
[15] M.A. Azeez, A. Lateef, T.B. Asafa, T.A. Yekeen, A. Akinboro, I.C. Oladipo, E.B. Gueguim-Kana, L.S. Beukes, Biomedical applications of cocoa bean extract-mediated silver nanoparticles as antimicrobial, larvicidal and anticoagulant agents, J. Cluster Sci. 28 (2017) 149–164, https://doi.org/10.1007/s10876-016-1055-2.
[16] A.E. Adebayo, A.M. Oke, A. Lateef, A.A. Oyatokun, O.D. Abisoye, I.P. Adiji, D.O. Fagbenro, T.V. Amusan, J.A. Badmus, T.B. Asafa, L.S. Beukes, E.B. Gueguim-Kana, S.H. Abbas, Biosynthesis of silver, gold and silver–gold alloy nanoparticles using Persea americana fruit peel aqueous extract for their biomedical properties, Nanotechnol. Environ. Eng. 4 (2019) 1–15, https://doi.org/10.1007/s41204-019-0060-8.
[17] M.S. Bethu, V.R. Netala, L. Domdi, V. Tartte, V.R. Janapala, Potential anticancer activity of biogenic silver nanoparticles using leaf extract of Rhynchosia suaveolens: an insight into the mechanism, Artif. Cell Nanomed. Biotechnol. (2018) 1–11, https://doi.org/10.1080/21691401.2017.1414824, 0.
[18] S. Majeed, M.S. bin Abdullah, A. Nanda, M.T. Ansari, In vitro study of the antibacterial and anticancer activities of silver nanoparticles synthesized from Penicillium brevicompactum (MTCC-1999), J. Taibah Univ. Sci. 10 (2016) 614–620, https://doi.org/10.1016/j.jtusci.2016.02.010.
[19] M. Naz, N. Nasiri, M. Ikram, M. Nafees, M.Z. Qureshi, S. Ali, A. Tricoli, Eco-friendly biosynthesis, anticancer drug loading and cytotoxic effect of capped Ag-nanoparticles against breast cancer, Appl. Nanosci. 7 (2017) 793–802, https://doi.org/10.1007/s13204-017-0615-6.
[20] K. Venugopal, H.A. Rather, K. Rajagopal, M.P. Shanthi, K. Sheriff, M. Illiyas, R.A. Rather, E. Manikandan, S. Uvarajan, M. Bhaskar, M. Maaza, Synthesis of silver nanoparticles (Ag NPs) for anticancer activities (MCF 7 breast and A549 lung cell lines) of the crude extract of Syzygium aromaticum, J. Photochem. Photobiol. B Biol. 167 (2017) 282–289, https://doi.org/10.1016/j.jphotobiol.2016.12.013.
[21] M. Kooti, A.N. Sedeh, H. Motamedi, S.E. Rezatofighi, Magnetic graphene oxide inlaid with silver nanoparticles as antibacterial and drug delivery composite, Appl. Microbiol. Biotechnol. 102 (2018) 3607–3621, https://doi.org/10.1007/s00253-018-8880-1.
[22] L. Wang, C. Hu, L. Shao, The antimicrobial activity of nanoparticles: present situation and prospects for the future, Int. J. Nanomed. 12 (2017) 1227–1249, https://doi.org/10.2147/IJN.S121956.

[23] G.V. Vimbela, S.M. Ngo, C. Fraze, L. Yang, D.A. Stout, Antibacterial properties and toxicity from metallic nanomaterials, Int. J. Nanomed. 12 (2017) 3941–3965, https://doi.org/10.2147/IJN.S134526.
[24] A. Jung, Y. Jik, " Nanoantibiotics " : a new paradigm for treating infectious diseases using nanomaterials in the antibiotics resistant era, J. Contr. Release 156 (2011) 128–145, https://doi.org/10.1016/j.jconrel.2011.07.002.
[25] J. Kim, S. Kwon, E. Ostler, Antimicrobial effect of silver-impregnated cellulose: potential for antimicrobial therapy, J. Biol. Eng. 3 (2009) 1–9, https://doi.org/10.1186/1754-1611-3-20.
[26] I. V Voznyĭ, I.S. Lukomskaia, I.M. Lanskaia, E.I. Podkidysheva, Synthesis of beta-maltosides, derivatives of p-nitrophenol, 2-chloro-4-nitrophenol, and 4-methylumbelliferone, and their use as substrates for determining alpha-glucosidase activity, Vopr. Med. Khim. 42 (1996) 348–354. http://www.ncbi.nlm.nih.gov/pubmed/9254525. (Accessed 29 March 2020).
[27] Q.L. Zhu, Q. Xu, Immobilization of ultrafine metal nanoparticles to high-surface-area materials and their catalytic applications, Chem 1 (2016) 220–245, https://doi.org/10.1016/j.chempr.2016.07.005.
[28] M.M. Khin, A.S. Nair, V.J. Babu, R. Murugan, S. Ramakrishna, A review on nanomaterials for environmental remediation, Energy Environ. Sci. 5 (2012) 8075–8109, https://doi.org/10.1039/c2ee21818f.
[29] S. Taghipour, S.M. Hosseini, B. Ataie-Ashtiani, Engineering nanomaterials for water and wastewater treatment: review of classifications, properties and applications, New J. Chem. 43 (2019) 7902–7927, https://doi.org/10.1039/c9nj00157c.
[30] I. Ali, New generation adsorbents for water treatment, Chem. Rev. 112 (2012) 5073–5091, https://doi.org/10.1021/cr300133d.
[31] T. Chen, W. Quan, L. Yu, Y. Hong, C. Song, M. Fan, L. Xiao, W. Gu, W. Shi, One-step synthesis and visible-light-driven H2 production from water splitting of Ag quantum dots/g-C3N4 photocatalysts, J. Alloys Compd. 686 (2016) 628–634, https://doi.org/10.1016/j.jallcom.2016.06.076.
[32] M.A. Ebrahimzadeh, A. Naghizadeh, O. Amiri, M. Shirzadi-Ahodashti, S. Mortazavi-Derazkola, Green and facile synthesis of Ag nanoparticles using Crataegus pentagyna fruit extract (CP-AgNPs) for organic pollution dyes degradation and antibacterial application, Bioorg. Chem. 94 (2020) 103425, https://doi.org/10.1016/j.bioorg.2019.103425.
[33] D. Jiang, J. Xie, M. Chen, D. Li, J. Zhu, H. Qin, Facile route to silver submicron-sized particles and their catalytic activity towards 4-nitrophenol reduction, J. Alloys Compd. 509 (2011) 1975–1979, https://doi.org/10.1016/j.jallcom.2010.10.107.
[34] Y. Fu, T. Huang, L. Zhang, J. Zhu, X. Wang, Ag/g-C3N4 catalyst with superior catalytic performance for the degradation of dyes: a borohydride-generated superoxide radical approach, Nanoscale 7 (2015) 13723–13733, https://doi.org/10.1039/c5nr03260a.
[35] K. Tedsree, T. Li, S. Jones, C.W.A. Chan, K.M.K. Yu, P.A.J. Bagot, E.A. Marquis, G.D.W. Smith, S.C.E. Tsang, Hydrogen production from formic acid decomposition at room temperature using a Ag-Pd core-shell nanocatalyst, Nat. Nanotechnol. 6 (2011) 302–307, https://doi.org/10.1038/nnano.2011.42.
[36] A. Zhou, J. Li, G. Wang, Q. Xu, Preparation of Ag/ZrGP nanocomposites with enhanced catalytic activity for catalytic reduction of 4-nitrophenol, Appl. Surf. Sci. 506 (2020) 144570, https://doi.org/10.1016/j.apsusc.2019.144570.
[37] Z. Zhang, W. Shen, J. Xue, Y. Liu, Y. Liu, P. Yan, J. Liu, J. Tang, Recent advances in synthetic methods and applications of silver nanostructures, Nanoscale Res. Lett. 13 (2018) 1–18, https://doi.org/10.1186/s11671-018-2450-4.
[38] A. Lateef, M.A. Akande, M.A. Azeez, S.A. Ojo, B.I. Folarin, E.B. Gueguim-Kana, L.S. Beukes, Phytosynthesis of silver nanoparticles (AgNPs) using miracle fruit plant (Synsepalum dulcificum) for antimicrobial, catalytic, anticoagulant, and thrombolytic applications, Nanotechnol. Rev. 5 (2016) 507–520, https://doi.org/10.1515/ntrev-2016-0039.
[39] A. Lateef, S.A. Ojo, M.A. Azeez, T.B. Asafa, T.A. Yekeen, A. Akinboro, I.C. Oladipo, E.B. Gueguim-Kana, L.S. Beukes, Cobweb as novel biomaterial for the green and eco-friendly synthesis of silver nanoparticles, Appl. Nanosci. 6 (2016) 863–874, https://doi.org/10.1007/s13204-015-0492-9.
[40] A. Lateef, S.A. Ojo, J.A. Elegbede, The emerging roles of arthropods and their metabolites in the green synthesis of metallic nanoparticles, Nanotechnol. Rev. 5 (2016) 601–622, https://doi.org/10.1515/ntrev-2016-0049.
[41] I.A. Adelere, A. Lateef, A novel approach to the green synthesis of metallic nanoparticles: the use of agro-wastes, enzymes, and pigments, Nanotechnol. Rev. 5 (2016) 567–587, https://doi.org/10.1515/ntrev-2016-0024.
[42] S. Ahmed, M. Ahmad, B.L. Swami, S. Ikram, A review on plants extract mediated synthesis of silver nanoparticles for antimicrobial applications: a green expertise, J. Adv. Res. 7 (2016) 17–28, https://doi.org/10.1016/j.jare.2015.02.007.
[43] F.K. Alsammarraie, W. Wang, P. Zhou, A. Mustapha, M. Lin, Green synthesis of silver nanoparticles using turmeric extracts and investigation of their antibacterial activities, Colloids Surf. B Biointerfaces 171 (2018) 398–405, https://doi.org/10.1016/j.colsurfb.2018.07.059.
[44] M. Khatami, N. Zafarnia, M. Heydarpoor Bami, I. Sharifi, H. Singh, Antifungal and antibacterial activity of densely dispersed silver nanospheres with homogeneity size which synthesized using chicory: an in vitro study, J. Mycol. Med. 28 (2018) 637–644, https://doi.org/10.1016/j.mycmed.2018.07.007.
[45] S.G. Ali, M.A. Ansari, H.M. Khan, M. Jalal, A.A. Mahdi, S.S. Cameotra, Antibacterial and antibiofilm potential of green synthesized silver nanoparticles against imipenem resistant clinical isolates of P. aeruginosa, Bionanoscience 8 (2018) 544–553, https://doi.org/10.1007/s12668-018-0505-8.
[46] S. Eckhardt, P.S. Brunetto, J. Gagnon, M. Priebe, B. Giese, K.M. Fromm, Nanobio silver: its interactions with peptides and bacteria, and its uses in medicine, Chem. Rev. 113 (2013) 4708–4754, https://doi.org/10.1021/cr300288v.
[47] S. Pal, Y.K. Tak, J.M. Song, Does the antibacterial activity of silver nanoparticles depend on the shape of the nanoparticle? A study of the gram-negative bacterium Escherichia coli, Appl. Environ. Microbiol. 73 (2007) 1712–1720, https://doi.org/10.1128/AEM.02218-06.
[48] B. Lesiak, N. Rangam, P. Jiricek, I. Gordeev, J. Tóth, L. Kövér, M. Mohai, P. Borowicz, Surface study of Fe3O4 nanoparticles functionalized with biocompatible adsorbed molecules, Front. Chem. 7 (2019) 642, https://doi.org/10.3389/fchem.2019.00642.
[49] S. Nakamura, M. Sato, Y. Sato, N. Ando, T. Takayama, M. Fujita, M. Ishihara, Synthesis and application of silver nanoparticles (Ag nps) for the prevention of infection in healthcare workers, Int. J. Mol. Sci. 20 (2019), https://doi.org/10.3390/ijms20153620.
[50] V. Lavakumar, K. Masilamani, V. Ravichandiran, N. Venkateshan, D.V.R. Saigopal, C.K. Ashok Kumar, C. Sowmya, Promising upshot of silver nanoparticles primed from Gracilaria crassa against bacterial pathogens, Chem. Cent. J. 9 (2015) 42, https://doi.org/10.1186/s13065-015-0120-5.
[51] B. Ajitha, Y. Ashok Kumar Reddy, P. Sreedhara Reddy, Green synthesis and characterization of silver nanoparticles using Lantana camara leaf extract, Mater. Sci. Eng. C 49 (2015) 373–381, https://doi.org/10.1016/j.msec.2015.01.035.
[52] C. Xue, G.S. Métraux, J.E. Millstone, C.A. Mirkin, Mechanistic study of photomediated triangular silver nanoprism growth, J. Am. Chem. Soc. 130 (2008) 8337–8344, https://doi.org/10.1021/ja8005258.
[53] S. Ju, W.-T. Han, Effect of gamma-ray irradiation on the growth of Au nanoparticles embedded in the germano-silicate glass cladding of the silica glass fiber and its surface plasmon resonance response, Sensors 19 (2019) 1666, https://doi.org/10.3390/s19071666.
[54] V.I. Zakomirnyi, Z. Rinkevicius, G.V. Baryshnikov, L.K. Sørensen, H. Ågren, Extended discrete interaction model: plasmonic excitations of silver nanoparticles, J. Phys. Chem. C 123 (2019) 28867–28880, https://doi.org/10.1021/acs.jpcc.9b07410.
[55] Y. Sun, Y. Xia, Gold and silver nanoparticles: a class of chromophores with colors tunable in the range from 400 to 750 nm, Analyst 128 (2003) 686–691, https://doi.org/10.1039/b212437h.
[56] J. Nelayah, M. Kociak, O. Stéphan, F.J.G. De Abajo, M. Tencé, L. Henrard, D. Taverna, I. Pastoriza-Santos, L.M. Liz-Marzán, C. Colliex, Mapping surface plasmons on a single metallic nanoparticle, Nat. Phys. 3 (2007) 348–353, https://doi.org/10.1038/nphys575.
[57] Y.A. Krutyakov, A.A. Kudrinskiy, A.Y. Olenin, G.V. Lisichkin, Synthesis and properties of silver nanoparticles: advances and prospects, Russ. Chem. Rev. 77 (2008) 233–257, https://doi.org/10.1070/rc2008v077n03abeh003751.
[58] V. Amendola, O.M. Bakr, F. Stellacci, A study of the surface plasmon resonance of silver nanoparticles by the discrete dipole approximation method: effect of shape, size, structure, and assembly, Plasmonics 5 (2010) 85–97, https://doi.org/10.1007/s11468-009-9120-4.
[59] V.C. Karade, S.B. Parit, V.V. Dawkar, R.S. Devan, R.J. Choudhary, V.V. Kedge, N.V. Pawar, J.H. Kim, A.D. Chougale, A green approach for the synthesis of α-Fe2O3 nanoparticles from Gardenia resinifera plant and it's in vitro hyperthermia application, Heliyon 5 (2019), e02044, https://doi.org/10.1016/j.heliyon.2019.e02044.
[60] M. José Yacamán, J.A. Ascencio, H.B. Liu, J. Gardea-Torresdey, Structure shape and stability of nanometric sized particles, in: J. Vac. Sci. Technol. B Microelectron. Nanom. Struct., American Vacuum Society, 2001, pp. 1091–1103, https://doi.org/10.1116/1.1387089.
[61] J.R. Morones, J.L. Elechiguerra, A. Camacho, K. Holt, J.B. Kouri, J.T. Ramírez, M.J. Yacaman, JN2005, Nanotechnology 16 (2005) 2346–2353, https://doi.org/10.1088/0957-4484/16/10/059.
[62] C. Malarkodi, S. Rajeshkumar, K. Paulkumar, G.G. Jobitha, M. Vanaja, G. Annadurai, Biosynthesis of semiconductor nanoparticles by using sulfur reducing bacteria Serratia nematodiphila, Adv. Nano Res. 1 (2013) 83–91, https://doi.org/10.12989/anr.2013.1.2.083.
[63] M.G. Méndez-Medrano, E. Kowalska, M. Endo-Kimura, K. Wang, B. Ohtani, D. Bahena Uribe, J.L. Rodríguez-López, H. Remita, Inhibition of fungal growth using modified TiO2 with Core@Shell structure of Ag@CuO clusters, ACS Appl. Bio Mater. (2019), https://doi.org/10.1021/acsabm.9b00707.
[64] B. Reidy, A. Haase, A. Luch, K.A. Dawson, I. Lynch, Mechanisms of silver nanoparticle release, transformation and toxicity: a critical review of current knowledge and recommendations for future studies and applications, Materials (Basel) 6 (2013) 2295–2350, https://doi.org/10.3390/ma6062295.
[65] J. Li, K. Rong, H. Zhao, F. Li, Z. Lu, R. Chen, Highly selective antibacterial activities of silver nanoparticles against bacillus subtilis, J. Nanosci. Nanotechnol. 13 (2013) 6806–6813, https://doi.org/10.1166/jnn.2013.7781.
[66] T.L. Collins, E.A. Markus, D.J. Hassett, J.B. Robinson, The effect of a cationic porphyrin on pseudomonas aeruginosa biofilms, Curr. Microbiol. 61 (2010) 411–416, https://doi.org/10.1007/s00284-010-9629-y.
[67] A.A. El-Kheshen, S.F.G. El-Rab, Effect of reducing and protecting agents on size of silver nanoparticles and their anti-bacterial activity, Der Pharma Chem. 4 (2012) 53–65.
[68] M. Taner, N. Sayar, I.G. Yulug, S. Suzer, Synthesis, characterization and antibacterial investigation of silver-copper nanoalloys, J. Mater. Chem. 21 (2011) 13150–13154, https://doi.org/10.1039/c1jm11718a.

[69] S. Agnihotri, S. Mukherji, S. Mukherji, Size-controlled silver nanoparticles synthesized over the range 5-100 nm using the same protocol and their antibacterial efficacy, RSC Adv. 4 (2014) 3974–3983, https://doi.org/10.1039/c3ra44507k.
[70] M. Raffi, F. Hussain, T.M. Bhatti, J.I. Akhter, A. Hameed, M.M. Hasan, Antibacterial Characterization of Silver Nanoparticles against E. Coli ATCC-15224, 2008.
[71] T.C. Dakal, A. Kumar, R.S. Majumdar, V. Yadav, Mechanistic basis of antimicrobial actions of silver nanoparticles, Front. Microbiol. 7 (2016), https://doi.org/10.3389/fmicb.2016.01831.
[72] J.S. Kim, E. Kuk, K.N. Yu, J.H. Kim, S.J. Park, H.J. Lee, S.H. Kim, Y.K. Park, Y.H. Park, C.Y. Hwang, Y.K. Kim, Y.S. Lee, D.H. Jeong, M.H. Cho, Antimicrobial effects of silver nanoparticles, Nanomed. Nanotechnol. Biol. Med. 3 (2007) 95–101, https://doi.org/10.1016/j.nano.2006.12.001.
[73] A.S. Hashimi, M.A.N.M. Nohan, S.X. Chin, S. Zakaria, C.H. Chia, Rapid catalytic reduction of 4-nitrophenol and clock reaction of methylene blue using copper nanowires, Nanomaterials 9 (2019), https://doi.org/10.3390/nano9070936.
[74] S. Saha, A. Pal, S. Kundu, S. Basu, T. Pal, Photochemical green synthesis of calcium-alginate-stabilized ag and au nanoparticles and their catalytic application to 4-nitrophenol reduction, Langmuir 26 (2010) 2885–2893, https://doi.org/10.1021/la902950x.